JURNAL INFOTEL
VOL. 16, NO. 2, MAY 2024, PP. 457–473. DOI:10.20895/INFOTEL.V16I2.1118

RESEARCH ARTICLE

A Bandwidth and Gain Enhanced Hexagonal Patch Antenna using Hexagonal Shape SRR

Harfan Hian Ryanu[1,*], Syahna Hafizha[2], Azka Maulani[3], Aloysius Adya Pramudita[4], Bambang Setia Nugroho[5], Levy Olivia Nur[6], Rina Pudji Astuti[7], and Dwiyanto[8]

[1,2,3,4,5,6,7]Fakultas Teknik Elektro, Universitas Telkom, Bandung 40257, Indonesia
[8]Satellite Technology Research Center, National Research and Innovation Agency, Bogor 16310, Indonesia

*Corresponding email: harfanhr@telkomuniversity.ac.id

Received: December 31, 2023; Revised: February 4, 2024; Accepted: February 9, 2024.

Abstract: In the evolving digital era, the primary focus of the telecommunications industry is on the 5G network, which is expected to deliver high data rates, low latency, large network capacity, and improved connectivity. This article discusses efforts to adopt optimal frequencies for 5G, introducing techniques to enhance the characteristics of microstrip antennas using double negative (DNG) metamaterial properties. The hexagonal-shaped split ring resonant (HSRR) metamaterial is a potential method to increase the bandwidth and gain of 5G antennas. Simulation of HSRR unit cells shows a positive impact on DNG characteristics. Meanwhile, the antenna design incorporating HSRR superstrate elements significantly increases gain to 4.47 dBi, and the implementation of HSRR structures on the ground plane results in a remarkable 368 % increase in bandwidth compared to conventional antennas without metamaterial.

Keywords: double negative metamaterial, hexagonal shaped SRR, metamaterial, 5G antennas.

1 Introduction

The need for fast and reliable connectivity is increasing in the continuously evolving digital era. Mobile communication technology has undergone rapid evolution from generation to

 ISSN: 2085-3688; e-ISSN: 2460-0997

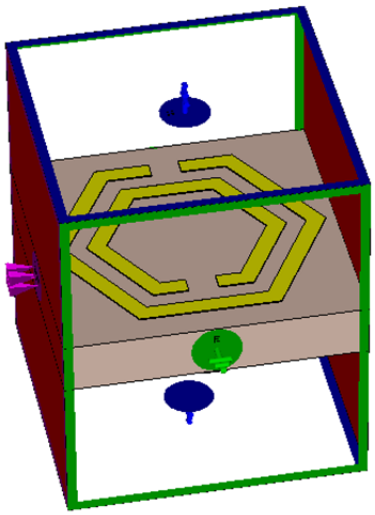

Figure 1: Unit cell simulation.

generation, and currently, 5G networks have become the main focus in the telecommunications industry. Anticipated benefits of 5G services include delivering exceptionally high data rates (reaching up to 10 Gbps for downlink and 20 Gbps for uplink), minimal latency (below 1 ms), increased network capacity, and enhanced connectivity, all designed to fulfill the requirements of contemporary society [1]. There are three categories of 5G use cases: enhanced mobile broadband (eMBB) catering to high-speed broadband connectivity, ultra-reliable low latency communication (URLLC) designed for mission-critical communication, particularly in emergencies such as disasters, and Massive IoT (MioT) facilitating connection of millions of devices within a specific area [2]. Various efforts have been made to adopt the most optimal frequency bands for 5G utilization. The 3rd Generation Partnership Project (3GPP) divides the 5G bands into two groups: Frequency Range 1 (FR1) for bands up to 7.125 GHz, and Frequency Range 2 (FR2) for bands above 24.25 GHz. Based on its propagation characteristics, these frequency bands can be grouped into three [3,4]:

1. Low band spectrum (< 2 GHz) is a band used to provide wide coverage, especially in rural areas. This spectrum range has the lowest bandwidth channels compared to other bands with a maximum of 20 MHz bandwidth.
2. Spectrum mid band (3-6 GHz) is used for high data speeds and has attractive propagation characteristics to support small cell services. In this band, there are N77 and N78 bands with a frequency range of 3300 - 4200 MHz, which are accepted globally.
3. Spectrum high band (> 24 GHz) is a breakthrough in 5G services that supports superior data rates with the trade-off of low coverage. This band is suitable for hotspot coverage needs and is supported by an average bandwidth channel of 400 MHz, with the largest channel being 2 GHz [5].

Antennas that are used to meet the needs of various 5G services must have a wide bandwidth so that they can support high-speed services but remain small and light in size to support mobility on the mobile terminal side. Microstrip antennas generally have small

dimensions but with narrow bandwidth. On the other hand, microstrip antennas also have a low gain. Multiple antenna elements can be used to overcome this problem, but such a method results in increasing complexity of the antenna design, and thus the number of excitations used [6, 7].

Several techniques have been reported to be used to improve the characteristics of microstrip antennas. The defected ground structure (DGS) technique is a popular technique used to increase antenna bandwidth [8–10]. In the DGS technique, the antenna ground plane is partially removed, thereby reducing surface wave propagation on the ground plane. However, reducing surface waves also has a negative effect on antenna gain and gives rise to backside radiation [11]. The dual-mode resonance method can reportedly be used to produce high antenna gain with increased bandwidth [12–14]. Such a method uses a pair of slots to induce capacitance to control dual resonant frequencies. However, generally, each resonant mode has a slightly different frequency [13]. Alternatively, substrate integrated waveguide (SIW) can also be used to increase the bandwidth and gain characteristics of the antenna [15–17]. However, they have a very complex and high-profile design.

Table 1: Antenna specification

Antenna Parameter	**Detail Specification**
Center frequency	5G Band (3.5 GHz)
Bandwidth	3.3 - 3.8 GHz (N78 Band)
S_{11}	< -10 dB
Gain improvement	> 1 dBi
Radiation pattern	Unidirectional

Metamaterials are a promising method for improving the characteristics of microstrip antennas [18–25]. Metamaterial is a man-made material that consists of a certain structural arrangement of conductor on the surface of its dielectric substrate which gives the effect of negative permittivity (ε) and/or permeability (μ) values [21]. The structure is arranged in such a way that it provides various effects such as miniaturization [25], increased bandwidth [19, 21], gain [22, 24], and mutual coupling [26] of the antenna. Split ring resonant (SRR) is one metamaterial with a structure that consists of two rings (called outer and inner). A gap is placed at the bottom of the inner and top of the outer. SRR possesses attributes akin to a double negative metamaterial (DNG), commonly known as a left-handed metamaterial (LHM). It demonstrates distinctive electromagnetic properties, including a negative refraction index, along with simultaneously negative values for permeability and permittivity. SRR can be combined on the ground plane of the antenna or as an additional superstrate layer at the top of the antenna.

This paper discusses the method of increasing antenna bandwidth and gain by utilizing hexagonal-shaped SRR (HSRR) unit cells. The unit cells are arranged in two positions: as a superstrate and on the ground plane respectively. A simulation of the unit cell was conducted to examine the properties of DNG within the cell. The FR-4 Epoxy substrate material with ε_r = 4.4 and thickness 1.6 mm is utilized in the design of the antenna. The antenna design results show that the addition of a superstrate element with a full HSRR configuration has the greatest impact on increasing gain. Meanwhile, the implementation

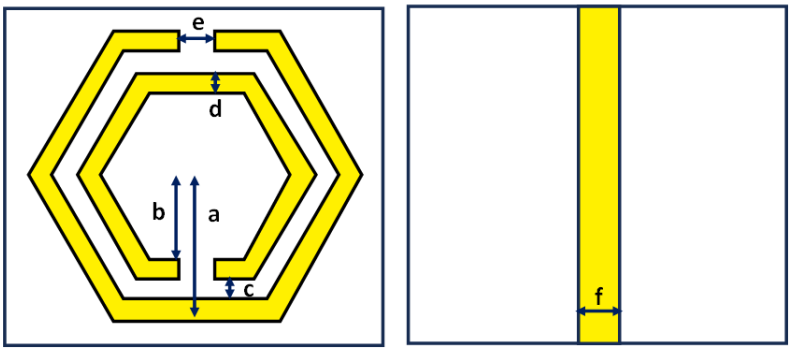

Figure 2: Unit cell geometry front side (left) back side (right).

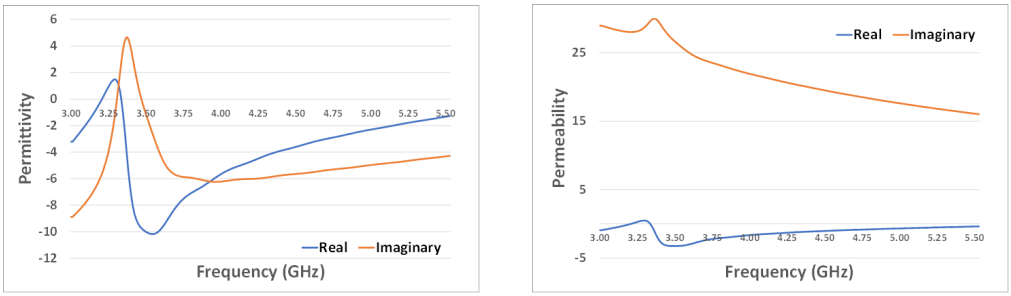

(a) (b)

Figure 3: Result of permittivity and permeability extraction of unit cell from material (a) permittivity (b) permeability.

of the HSRR unit sell structure on the ground plane is able to increase the bandwidth by up to 368 % of conventional antennas without a metamaterial structure.

2 Design of Metamaterial Antenna

2.1 Proposed Antenna Specification

Table 1 shows the design specifications of the target antenna. The designed antenna uses band N 78 in the 3.5 GHz frequency band for 5G technology. with a bandwidth of 500 MHz from 3.3 to 3.8 GHz. The objective of augmenting gain through the utilization of metamaterial is set larger than 1 dB. The aspired enhancement in gain is deliberately constrained, considering the inherent limitations of microstrip antenna characteristics. Microstrip antennas inherently exhibit low gain, in stark contrast to aperture antennas. Nevertheless, this study still aims to observe the extent to which the inclusion of metamaterial can impact the gain of the antenna.

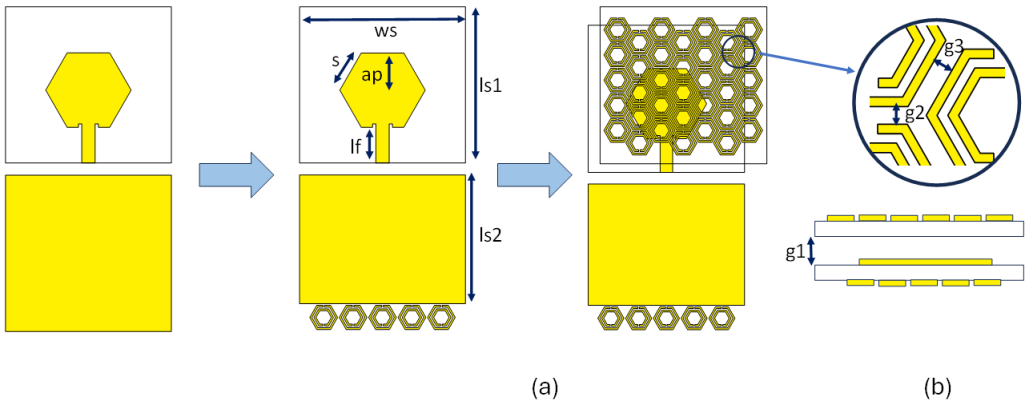

Figure 4: Antenna design and geometry (a) process design of the proposed antenna (top view: patch and bottom view: ground plane) (b) positioning of the antenna and superstrate.

Table 2: Antenna geometry and dimension

Parameter	**ws**	**ls**	**ls1**	**s**	**ap**	**lf**	**g1**	**g2**	**g3**	**a**	**b**
Value (mm)	55	55	39.21	15.6	13.51	9.22	10	0.75	1.5	4.34	2.4
Parameter (Cont.)	**c**	**d**	**e**	**f**							
Value (mm) (Cont.)	0.62	0.62	0.46	0.775							

2.2 Characterization of HSRR Unit Cell

To analyze the characteristics of DNG, a unit cell simulation was carried out by modeling a thin wire structure combined with a hexagonal SRR structure. The overall configuration is depicted in Figure 1. A hexagonal unit cell facing the Z+ axis is simulated with the Perfect Electric Conductor (PEC) boundary condition on the Y-axis side, and the Perfect Magnetic Conductor (PMC) on the Z-axis side. Two wave ports are used on the X-axis side of the unit cell [27]. As depicted in Figure 2, the radius of the hexagon outside ring (a) is 4.34 mm, the radius of the hexagon inside ring (b) is 2.48 mm, while the distance of the ring (c) and the thickness of the ring (d) both have the same value which is 0.62 mm. The split gap of the ring (e) and the width of the backside transmission line are 0.465 mm and 0.775 mm respectively.

After the process of simulation, S-Parameter measurements were carried out using the time domain solver. The permittivity and permeability values are then extracted from the S-Parameter using Chen's method [28]. Figure 3a and Figure 3b show the extraction results of permittivity and permeability respectively. It is depicted that the permittivity and permeability values for the cell unit are negative at the 3.5 GHz frequency, showing values of -10.05 and -3.24 respectively. This phenomenon exhibits the DNG characteristics of the proposed HSRR structure at the desired frequency band.

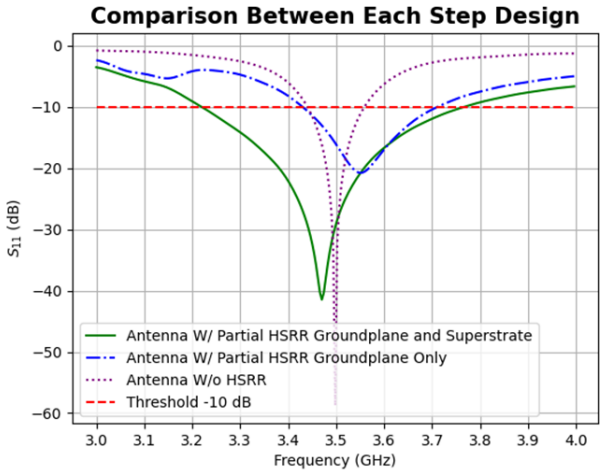

Figure 5: S_{11} comparison result between each step.

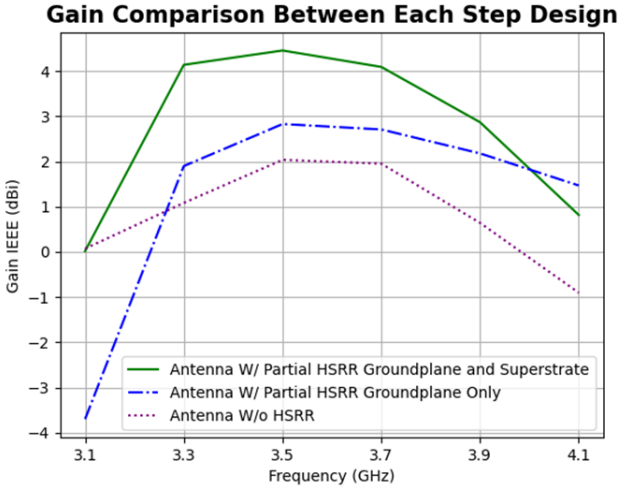

Figure 6: Gain comparison result between each step.

2.3 Antenna Design Process

The Antenna design process can be seen in Figure 4. The initial stage is designing a hexagonal patch antenna. The length of the hexagonal side (s) and the apothem value (ap) of the hexagonal patch can be found using (1) and (2) [29]:

$$S = \frac{c}{3.1033 f_r \sqrt{\epsilon_r}} \tag{1}$$

$$ap = \frac{\sqrt{3}}{2s} \tag{2}$$

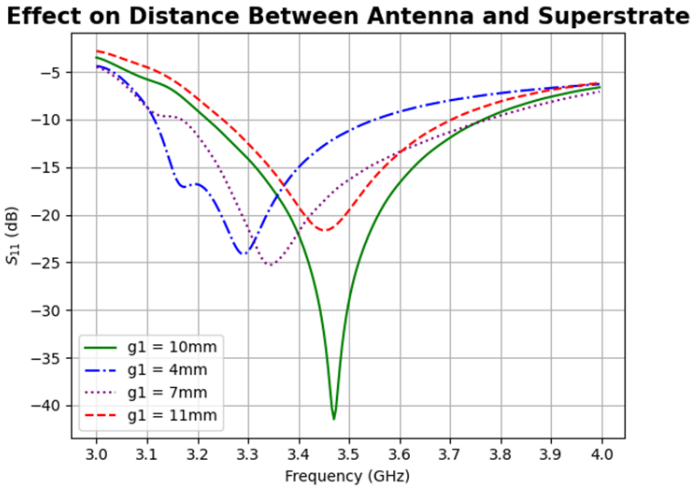

Figure 7: Effect on distance of antenna and superstrate to S_{11} parameter.

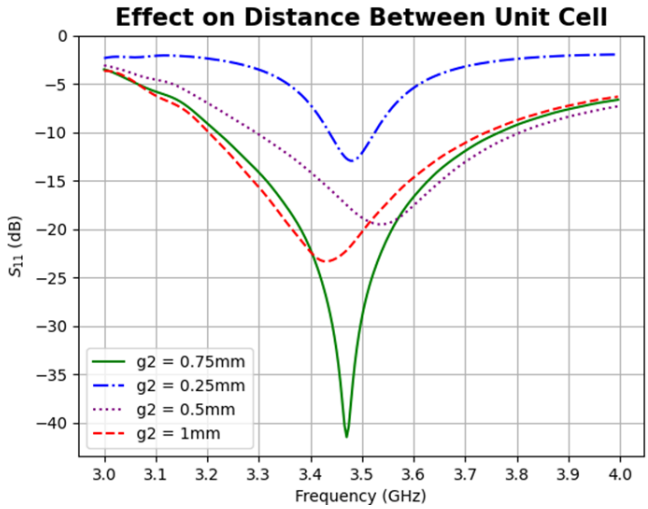

Figure 8: Effect on distance between unit cell to S_{11} parameter.

After the design of the first stage antenna was optimized, the HSRR structure was added in two stages, namely embedding the HSRR structure using a partial ground plane to increase the bandwidth, and the next stage is integrating the HSRR structure as a superstrate to increase the antenna gain. Each HSRR element is embedded carefully to obtain optimal values for each parameter and bandwidth. The proposed antenna's dimensional values are evident in Table 2. The antenna is simulated employing FR-4 Epoxy material with a permittivity value of ε_r = 4.4 and 1.6 mm thickness.

The simulation results of S_{11} parameters and gain from each design process can be observed in Figure 5 and Figure 6 respectively. From the picture it can be concluded that all

designed antennas exhibit an S_{11} below -10 dB at the central frequency of 3.5 GHz, thereby meeting the specifications in Table 1. Moreover, the addition of HSRR structures at each step influences both the bandwidth and the gain of the antenna. The antenna without the HSRR unit cell has a bandwidth of just 118 MHz and a gain of 2.01 dBi. By adding five HSRR elements at the bottom of the ground plane, there is an increase in bandwidth of 140 % and a gain of 0.83 dB to 283 MHz and 2.84 dBi respectively. Adding a superstrate structure further increases the bandwidth up to 368 % and gain up to 2.46 dB of the antenna without HSRR into a bandwidth of 552 MHz covering entirely 5G N78 band (3.3 – 3.8 GHz) and a gain of 4.47 dBi. This is due to as a DNG material, HSRR has negative refraction properties which can take advantage of electromagnetic waves coming from various directions. On the other hand, DNG metamaterial also acts as a lens that is able to focus the energy emitted from the antenna so that it can increase directivity and gain [30].

3 Result and Analysis

3.1 Parametric Studies of HSRR Element

To increase the understanding of the influence of SRR on antenna characteristics, a parametric study was carried out, namely the distance between the antenna and the superstrate (g1), and also the distance between the HSRR elements (g2). Changes in the parameter g1 can be observed in Figure 7 and have varying effects on the center frequency of the antenna. Although the increase in antenna bandwidth continues to occur in the 3.1 – 3.8 GHz frequency range, there is a shift in the center frequency. The closer the superstrate element is to the antenna, the smaller the center frequency value becomes.

At a distance g1=4mm, the center frequency is in the 3.29 GHz band, meanwhile, if g1 is increased to 13mm, the center frequency moves to the 3.48 GHz band. On the other hand, changes in the distance between elements (g2) have a direct effect on the bandwidth and return loss of the antenna. These results can be observed in Figure 8. Using a smaller g2 value of 0.25 mm, the S_{11} value is -12.93 dB, and a smaller bandwidth of 90 MHz, so it is necessary to adjust the impedance matching scheme from the antenna side. Meanwhile, by increasing the g2 value to 0.75 mm and 1 mm, the bandwidth and S_{11} values increase to above 500 MHz and above -20 dB respectively.

3.2 Influence of the quantity of HSRR metamaterial on antenna

The next step is to understand the effect of the number of H-SRRs on the superstrate on the antenna gain. In this research, three experiments were carried out, namely using 1 HSRR element, 10 HSRR elements, and full HSRR on the superstrate (35 HSRR elements). Simulation results in Figure 9 depict that the increase in antenna gain is equivalent to increasing the number of HSRR elements in the superstrate. By using 1 HSRR element the antenna gain increases to 2.49 dBi, then increasing to 10 HSRR elements increases the gain by 3.29 dBi. The use of 35 HSRR elements increases the gain to 4.47 dBi.

3.3 Antenna Fabrication and Measurement

After obtaining optimal simulations from the results of parametric studies and analysis of the number of HSRR elements, the next stage is to manufacture the antenna. The an-

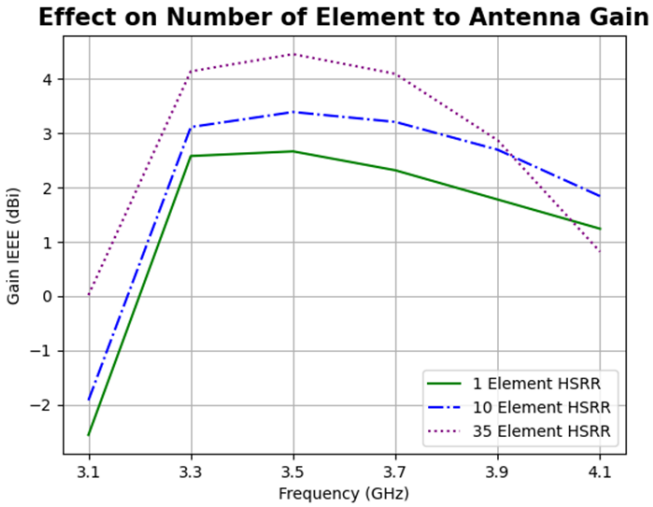

Figure 9: Effect on number of elements to antenna gain.

Table 3: Power link budget calculation

Known Parameter	Value	
	Antenna with Superstrate	Antenna without Superstrate
S_{21}	-44.471 dB	-46.955 dB
g_t	10.4 dBi	
L_{tx}	2.50 dB	
L_{rx}	3.00 dB	
FSL	52.86 dBm	
G_r	3.489 dBi	1.005 dBi

tenna is fabricated using FR-4 epoxy substrate material with a substrate thickness of 1.6 mm, relative permittivity of 4.4, and copper thickness of 0.035 mm. The final dimensions of the antenna are 55x55 mm2. The antenna manufacturing and S_{11} measurement results can be observed in Figure 10 and Figure 11, respectively. From Figure 11, several pieces of information can be obtained that for antennas without HSRR superstrate, the measurement results have characteristics that are almost similar to the simulation results but with a smaller bandwidth. The bandwidth measurement results show a value of 123 MHz, with the largest S_{11} in the 3.56 GHz frequency band being -24.94 dB, while the simulation results show a bandwidth value of 283 MHz with an S_{11} of -20.61 dB in the 3.56 GHz frequency band. On the other hand, adding the superstrate element significantly shifts the working frequency to a greater frequency for the measured antenna. The bandwidth where the S_{11} value is below -10 dB is in the 3.4 GHz to 3.8 GHz band. Thus, the measurement results of the proposed antenna have a bandwidth of 400 MHz, with the best S_{11} being in the 3.76 GHz band of -22.43 dB. This value is much shifted from the simulation results, namely with a bandwidth of 552 MHz, with the best S_{11} being in the 3.47 GHz frequency band of -40.30 dB. The frequency band shift is determined by the composition of the FR-4 sub-

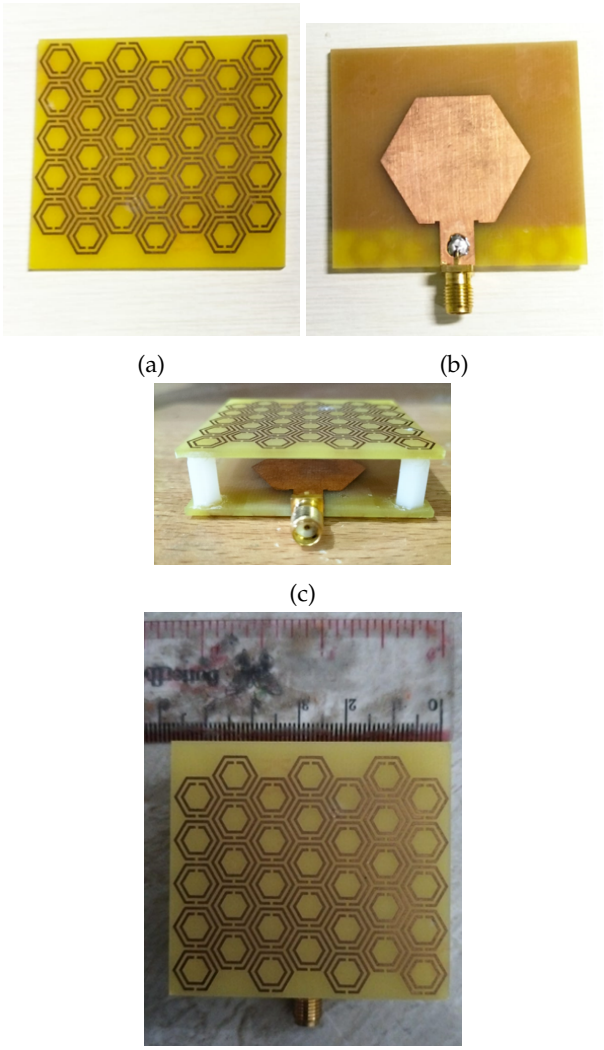

(a) (b)

(c)

(d)

Figure 10: Antenna fabrication result (a) superstrate element; (b) antenna element; (c) integration of antenna and superstrate; (d) the antenna size.

strate used during fabrication and the accuracy of the fabrication process itself, affecting the impedance bandwidth of the antenna.

The next stage is measuring the antenna radiation parameters, namely the gain and radiation pattern. Measurement of gain is using a vector network analyzer (VNA) and a horn antenna as a transmitter antenna by measuring the S_{21} parameters as gain and attenuation values contained in the antenna propagation channel using (3) and (4) [31].

$$S_{21} = P_r - P_t \tag{3}$$

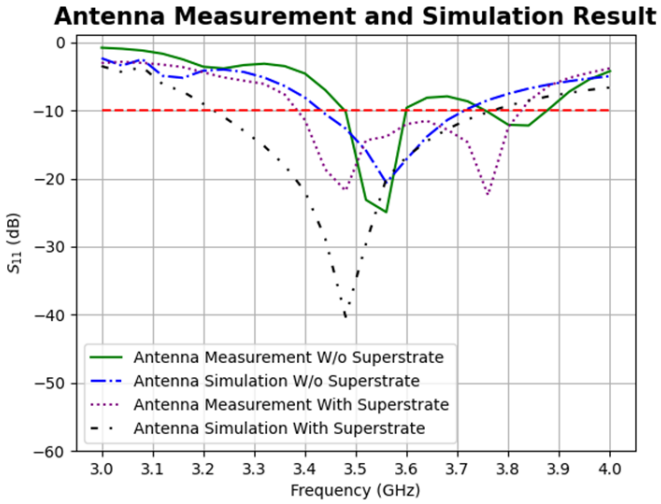

Figure 11: Antenna measurement result and simulation.

Table 4: Summary of bandwidth and gain for each design step of antenna

Design	Simulation		Measurement	
	BW(MHz)	Gain (dBi)	BW (MHz)	Gain (dBi)
Conventional Antenna	118	2.01	-	-
HSRR Groundplane	283	2.84	123	1.005
HSRR Groundplane and Superstrate	552	4.47	400	3.489

$$S_{21} = G_t + G_r - L_{tx} - L_{rx} - FSL \tag{4}$$

where P_t is transmitted power, P_r is received power, G_t is transmit antenna gain, L_{tx} is transmitter antenna cable attenuation, L_{rx} is receiver cable attenuation, and FSL is free space loss.

Because these values can be known, the G_r value or receiver gain can be measured via the S_{21} value read on the VNA. The VNA used in this measurement is VNA-T5280 with an operating frequency of 300 KHz - 8 GHz. The measurement process was carried out at the Anechoic Chamber in Telkom University, and the experimental setup can be seen

Table 5: Comparison with previous works

Ref	Method	Bandwidth Improvement (MHz)	Gain Improvement (dB)
[32]	Slot and Parasitic Stripe	20	1
[33]	Stacked Patch	326.5	-
[28]	CSRR	650	-
[34]	Metasurface Reflector	70	4.57
[35]	DGS and Horizontal Patch Gap	421.2	1.73
[8]	Slot and DGS	411	0.57
This Works	SRR DGS and Superstrate	400	3.49

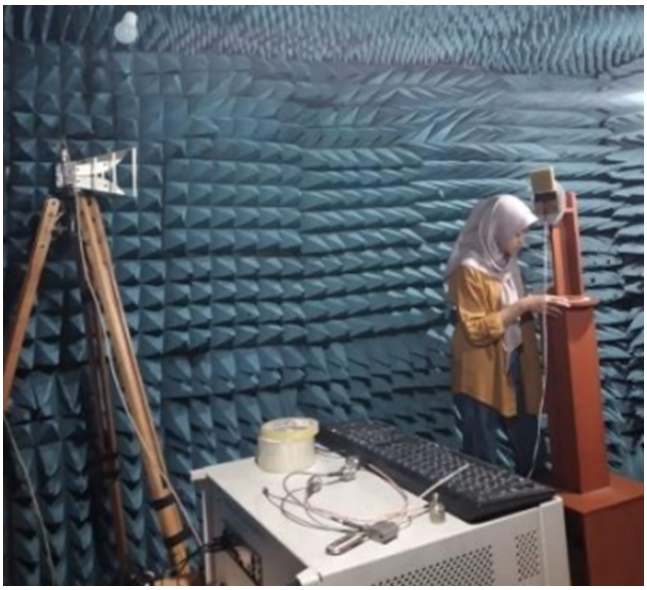

Figure 12: Experimental setup of the antenna measurement.

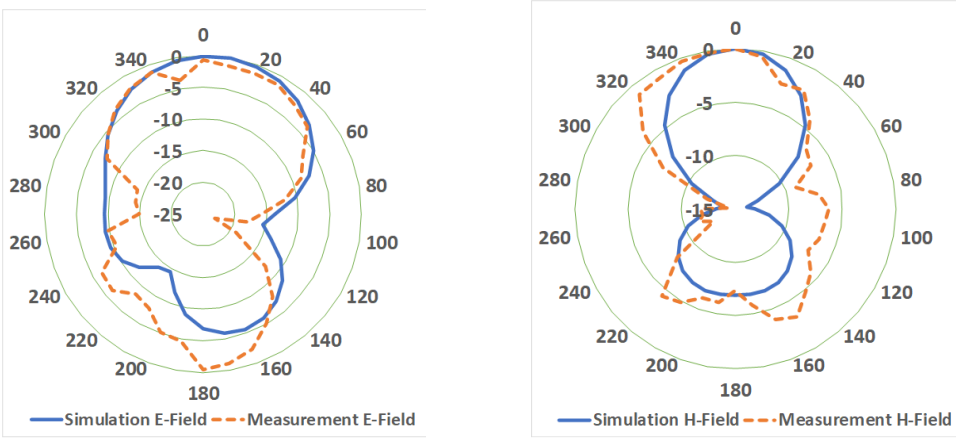

(a) (b)

Figure 13: Radiation pattern comparison between simulation and measurement (a) E-Plane (b) H-Plane.

in Figure 12. The Detailed power link budget parameter values above can be observed in Table 3. The measurement distance between the horn antenna and the antenna under test is 3 meters. According to the measurement results, it can be observed that the addition of the superstrate element increases the antenna gain by 2,484 dB from a value of 1,005 dBi to 3,489 dBi in the 3.5 GHz frequency band. This confirms the results of increasing the simulation gain by 2.01 dB by adding a superstrate element to the antenna. Meanwhile, the

slight differences that appear between the simulation and measurement results are caused by power fluctuations in the measurement results caused by reflections and noise in the measurement environment. Radiation pattern measurement utilizes the identical system applied for gain measurement. Yet, the testing antenna undergoes a comprehensive 360-degree rotation, spanning both the E-Plane and H-Plane directions. Figure 13 illustrates the observed radiation patterns in both planes. The acquired radiation pattern measurements corroborate the simulation results in both the E-plane and H-plane, revealing unidirectional characteristics. Nevertheless, a slight amplification in back lobe power is noticeable in the E-field measurement, attributable to power fluctuations originating from the indoor measurement environment.

4 Discussion

4.1 Comparison Between Each Design Step of Antenna Measurement and Simulation

Table 4 summarizes simulation and measurement results for each step of the antenna design process. The table indicates that the addition of HSRR to the ground plane has a significant impact on increasing the antenna bandwidth. Regarding simulation, there is a 140 % increase in bandwidth and a gain improvement of 0.84 dB. On the other hand, adding HSRR to the superstrate significantly affects both the bandwidth and gain of the antenna. In simulation, there is a 95 % increase in bandwidth and a gain improvement of 1.63 dB compared to the previous step. In measurements, there is a substantial increase in both bandwidth and gain, amounting to 225 % and 3.484 dB, respectively. The increase in bandwidth is attributed to the Negative Refraction Characteristic of the HSRR unit cell that enhances the impedance bandwidth of the antenna. On the other hand, the gain improvement results from the HSRR element in the superstrate serving as a lens and director, contributing to an enhancement in the antenna's directivity.

4.2 Comparison with Previous Works

In the final discussion phase, the proposed antenna design is compared with several prior studies on enhancing bandwidth and gain. This comparison considers antenna dimensions, employed methods, gain improvement, and bandwidth enhancement. Table 5 presents a comparative analysis, revealing that the proposed method exhibits a more pronounced influence on both bandwidth and gain when compared to alternative methods. Regarding bandwidth, the approach [28] offers a noteworthy increase, although it does not substantially affect antenna gain. Conversely, method [34] demonstrates a commendable gain improvement but does not significantly impact bandwidth. The proposed method yields a balanced and significant improvement in both gain and bandwidth based on the overall results.

5 Conclusion

This research has investigated the effect of an HSRR metamaterial structure on the bandwidth and gain of the antenna through two different configurations, namely the ground

plane section and the superstrate section. The antenna was designed using 3D modeler simulation software, and the manufacturing process was carried out after obtaining the most optimum results. The simulation results show that the superstrate with a complete HSRR configuration has the most significant gain increase impact of 4.47 dBi. Conversely, employing the HSRR unit cell configuration on the ground plane enhances the bandwidth to 552 MHz, representing a 368 % increase compared to a conventional antenna without a metamaterial structure. The suggested antenna operates at a frequency of 3.5 GHz, and the measurement outcomes align with the simulated results for both bandwidth and gain. Specifically, the measurements indicate a bandwidth of 400 MHz and a gain of 3.489 dBi.

6 Future Works

This study investigated the influence of HSRR metamaterial on the impedance bandwidth and gain of the antenna. In subsequent future works, further analysis can be conducted to explore additional impacts of the HSRR element on the antenna, such as the potential for antenna miniaturization, as well as possibilities related to beamforming and beam steering.

References

[1] R. P. Astuti, E. L. Wijaya, T. Yunita, and H. H. Ryanu, "Optimum polarization configuration of planar circular patch MIMO antenna," *J. Infotel*, vol. 14, pp. 20–29, Feb. 2022.

[2] B. S. Khan, S. Jangsher, A. Ahmed, and A. Al-Dweik, "Urllc and embb in 5g industrial iot: A survey," *IEEE Open Journal of the Communications Society*, vol. 3, pp. 1134–1163, 2022.

[3] P. S. M. Tripathi and R. Prasad, "Spectrum for 5G services," *Wirel. Pers. Commun.*, vol. 100, pp. 539–555, May 2018.

[4] O. O. Erunkulu, A. M. Zungeru, C. K. Lebekwe, M. Mosalaosi, and J. M. Chuma, "5g mobile communication applications: A survey and comparison of use cases," *IEEE Access*, vol. 9, pp. 97251–97295, 2021.

[5] E. Dahlman, S. Parkvall, and J. Skold, *5G NR: The Next Generation Wireless Access Technology*. Elsevier Science, 2020.

[6] G. Rai, "A survey: Antenna design structure for massive MIMO," *International Journal of Advanced and Innovative Research*, vol. 7, no. 2, pp. 79–81, 2018.

[7] P. W. Futter and J. Soler, "Antenna design for 5g communications," in *2017 Sixth Asia-Pacific Conference on Antennas and Propagation (APCAP)*, pp. 1–3, 2017.

[8] F. Y. Zulkifli and M. W. Iqbal, "Bandwidth and gain enhancement of microstrip leaky-wave antennas with slot and defected ground structure," *J. Eng. Technol. Sci.*, vol. 55, pp. 289–299, Aug. 2023.

[9] J.-I. Jung and J.-R. Yang, "5.8-GHz patch antenna with an enhanced defected ground structure for size reduction and increased bandwidth," *J Electromagn Eng Sci*, vol. 22, pp. 245–251, May 2022.

[10] R. Sahu, H. Pradhan, B. B. Mangaraj, and S. K. Behera, "Defected ground structure based compact UWB dielectric resonator antennas with enhanced bandwidth," *Frequenz*, vol. 77, pp. 537–548, Dec. 2023.

[11] C. Kumar and D. Guha, "Mitigating backside radiation issues of defected ground structure integrated microstrip patches," *IEEE Antennas Wirel. Propag. Lett.*, vol. 19, pp. 2502–2506, Dec. 2020.

[12] A. Bhattacharyya, J. Pal, K. Patra, and B. Gupta, "Bandwidth-enhanced miniaturized patch antenna operating at higher order dual-mode resonance using modal analysis," *IEEE Antennas Wirel. Propag. Lett.*, vol. 20, pp. 274–278, Feb. 2021.

[13] J. Wen, D. Xie, and L. Zhu, "Bandwidth-enhanced high-gain microstrip patch antenna under TM_{30} and TM_{50} dual-mode resonances," *IEEE Antennas Wirel. Propag. Lett.*, vol. 18, pp. 1976–1980, Oct. 2019.

[14] X. Zhang, T.-Y. Tan, Q.-S. Wu, L. Zhu, S. Zhong, and T. Yuan, "Pin-loaded patch antenna fed with a dual-mode SIW resonator for bandwidth enhancement and stable high gain," *IEEE Antennas Wirel. Propag. Lett.*, vol. 20, pp. 279–283, Feb. 2021.

[15] S. Liao, P. Chen, P. Wu, K. M. Shum, and Q. Xue, "Substrate-integrated waveguide-based 60-GHz resonant slotted waveguide arrays with wide impedance bandwidth and high gain," *IEEE Trans. Antennas Propag.*, vol. 63, pp. 2922–2931, July 2015.

[16] Y.-S. Huang, L. Zhou, Q.-H. Xu, and J.-F. Mao, "A w-band self-packaged SIW-based slot antenna with gain and bandwidth enhancement," *IEEE Trans. Antennas Propag.*, vol. 71, pp. 2158–2166, Mar. 2023.

[17] Y.-W. Wu, Z.-C. Hao, and Z.-W. Miao, "A planar *W*-band large-scale high-gain substrate-integrated waveguide slot array," *IEEE Trans. Antennas Propag.*, vol. 68, pp. 6429–6434, Aug. 2020.

[18] M. Hussain, W. A. Awan, M. S. Alzaidi, N. Hussain, E. M. Ali, and F. Falcone, "Metamaterials and their application in the performance enhancement of reconfigurable antennas: A review," *Micromachines (Basel)*, vol. 14, p. 349, Jan. 2023.

[19] H. A. Al Issa, Y. S. H. Khraisat, and F. A. S. Alghazo, "Bandwidth enhancement of microstrip patch antenna by using metamaterial," *Int. J. Interact. Mob. Technol.*, vol. 14, p. 169, Jan. 2020.

[20] V. Srinivasa Rao, K. V. V. S. Reddy, and A. M. Prasad, "Bandwidth enhancement of metamaterial loaded microstrip antenna using double layered substrate," *Indones. J. Electr. Eng. Comput. Sci.*, vol. 5, p. 661, Mar. 2017.

[21] H. H. Ryanu, M. Fadhil, and L. O. Nur, "A bandwidth enhanced circular ring microstrip antenna based on CSRR-loaded ground for 5G application," in *2023 IEEE International Conference on Industry 4.0, Artificial Intelligence, and Communications Technology (IAICT)*, IEEE, July 2023.

[22] B. A. F. Esmail, S. Koziel, and S. Szczepanski, "Overview of planar antenna loading metamaterials for gain performance enhancement: The two decades of progress," *IEEE Access*, vol. 10, pp. 27381–27403, 2022.

[23] C. M. Saleh, E. Almajali, A. Jarndal, J. Yousaf, S. S. Alja'Afreh, and R. E. Amaya, "Wideband 5G antenna gain enhancement using a compact single-layer millimeter wave metamaterial lens," *IEEE Access*, vol. 11, pp. 14928–14942, 2023.

[24] B. A. F. Esmail and S. Koziel, "Design and optimization of metamaterial-based 5G millimeter wave antenna for gain enhancement," *IEEE Trans. Circuits Syst. II Express Briefs*, vol. 70, pp. 3348–3352, Sept. 2023.

[25] S. A. Wicaksono, Edwar, H. H. Ryanu, B. S. Nugroho, and L. O. Nur, "Microstrip patch antenna miniaturization using metamaterial structure for 5G communication," in *5TH INTERNATIONAL CONFERENCE ON ELECTRICAL, ELECTRONIC, COMMUNICATION AND CONTROL ENGINEERING (ICEECC 2021)*, AIP Publishing, 2023.

[26] I. Nadeem and D.-Y. Choi, "Study on mutual coupling reduction technique for MIMO antennas," *IEEE Access*, vol. 7, pp. 563–586, 2019.

[27] A. Vallappil, B. Khawaja, M. Rahim, M. Iqbal, H. Chattha, and M. Ali, "A compact triple-band UWB inverted triangular antenna with dual-notch band characteristics using SSRR metamaterial structure for use in next-generation wireless systems," *Fractal Fract.*, vol. 6, p. 422, July 2022.

[28] H. H. Ryanu, M. Fadhil, and L. O. Nur, "A bandwidth enhanced circular ring microstrip antenna based on CSRR-loaded ground for 5G application," in *2023 IEEE International Conference on Industry 4.0, Artificial Intelligence, and Communications Technology (IAICT)*, IEEE, July 2023.

[29] K. Joshi, D. Yadav, and D. Bhardwaj, "Design of coplanar proximity coupled feed hexagonal shaped circular polarized microstrip patch antenna," *Trends in Sciences*, vol. 19, p. 4170, May 2022.

[30] S. Ranjeeta, K. Nitin, C. Gupta, S. Ranjeeta, K. Nitin, and C. Gupta, "Metamaterials for performance enhancement of patch antennas: A review," *Sci. Res. Essays*, vol. 9, pp. 43–47, Feb. 2014.

[31] D. C. Sianipar, L. Rafasari, H. H. Ryanu, B. S. Nugroho, and L. O. Nur, "Design and realization of metamaterial antenna for enhancement of antenna parameters in 5G frequency," *Journal of Measurements Electronics Communications and Systems*, vol. 10, p. 23, June 2023.

[32] S. K. Noor, M. Jusoh, T. Sabapathy, A. H. Rambe, H. Vettikalladi, A. M. Albishi, and M. Himdi, "A patch antenna with enhanced gain and bandwidth for sub-6 GHz and sub-7 GHz 5G wireless applications," *Electronics (Basel)*, vol. 12, p. 2555, June 2023.

[33] S. Pramono, M. H. Ibrahim, and M. B. Yunindanova, "Bandwidth enhancement using stacked patch MIMO antenna with low mutual coupling for 3.5 GHz," in *2019 6th International Conference on Information Technology, Computer and Electrical Engineering (ICITACEE)*, IEEE, Sept. 2019.

[34] M. Ameen, O. Ahmad, and R. K. Chaudhary, "Bandwidth and gain enhancement of triple-band MIMO antenna incorporating metasurface-based reflector for WLAN/WiMAX applications," *IET Microw. Antennas Propag.*, vol. 14, pp. 1493–1503, Oct. 2020.

[35] D. Rusdiyanto, C. Apriono, D. W. Astuti, and M. Muslim, "Bandwidth and gain enhancement of microstrip antenna using defected ground structure and horizontal patch gap," *Sinergi*, vol. 25, p. 153, Feb. 2021.